

**CHAPTER 1****THE SCREENED FIELD OF A TEST PARTICLE**

Robert L. Dewar

*Research School of Physics & Engineering  
The Australian National University  
Cenberra ACT 0200, Australia  
E-mail: robert.dewar@anu.edu.au*

The screened field (forward field and wake) of a test particle moving at constant velocity through an unmagnetized collisionless plasma is calculated analytically and numerically. This paper is based on unpublished material from my MSc thesis, supervised by the late Dr K. C. Hines.

**1. Introduction**

Interest in the kinetic theory of interacting charged particles at University of Melbourne developed from the work of Dr Ken Hines<sup>1</sup> in the 1950s—improving on a calculation by Landau<sup>2</sup> and using a formalism developed by Fano,<sup>3</sup> he calculated the slowing down distribution function of a charged “test particle” passing through a thin layer of material. The plasma theory group developing around Ken attracted a number of research students, including myself. The test particle diffusion problem provided a focus for a reading group on statistical physics<sup>4</sup> and plasma kinetic theory,<sup>5,6</sup> and research on the problem developed in several ways, including a relativistic generalization.<sup>7</sup>

The friction and diffusion coefficients of the Fokker–Planck equation suffer logarithmic divergences arising from the long-range nature of the Coulomb interaction. The fusion plasma theorists of the 1950s handled these divergences by the rather crude device of cutting off the interaction at the Debye length  $1/k_D$ , the characteristic length occurring in the screened electrostatic potential,  $q \exp(-k_D r)/r$ , in the neighbourhood of a static particle embedded in an ionized medium. While the logarithmic nature of the divergence makes the coefficients only weakly dependent on the

cutoff,<sup>7</sup> the *ad hoc* nature of this procedure was not very satisfactory from a fundamental point of view and this sparked research in the international theoretical physics community to find better approaches.

In 1960, using very sophisticated formalisms, Balescu<sup>8</sup> and Lenard<sup>9</sup> derived kinetic equations of the Landau form in which dynamical screening was incorporated through a frequency ( $\omega$ ) and wavenumber ( $\mathbf{k}$ ) dependent dielectric constant  $\epsilon(\omega, \mathbf{k})$ . The same Fokker–Planck–Landau equation (which is now known as the Balescu–Lenard equation) was derived by Thompson and Hubbard<sup>10,11,12</sup> from simpler statistical physics arguments in which the diffusion coefficient was calculated from a fluctuation spectrum obtained by superimposing the dielectrically screened fields of independently moving particles.

This approach was called the *dressed test particle picture* by Rostoker.<sup>13</sup> In this approach the unperturbed “test particles” replace the actual particles in the plasma. (In reality the trajectories are perturbed slightly by the fluctuations, giving rise to the linear dielectric response.)

The dressed test particle picture was developed in Fourier,  $(\omega, \mathbf{k})$ , representation rather than in real space-time,  $(\mathbf{x}, t)$ , and thus it was difficult to visualize the actual nature of the screened potential surrounding each particle. In Chapters 2 and 3 (unpublished) of my Master’s Thesis,<sup>14</sup> which was supervised by Ken Hines, I calculated the screened potential in real space for a nonrelativistic plasma.<sup>a</sup> This contribution to the K. C. Hines memorial volume is based on those chapters with only a few changes to make it self-contained and to improve readability.

For zero test particle velocity the solution is just the well-known Debye potential  $\exp(-k_D r)/r$ , but as the velocity is increased we may expect qualitative changes to occur. The work of Pines and Bohm<sup>16</sup> in which they considered forced vibrations of the collective coordinates indicates that for a particle moving slowly with respect to the electron thermal velocity the Debye potential is distorted into a set of spheroidal equipotentials centred on the particle and still decays exponentially with distance. We show that neither result is true, since the criterion  $k \lesssim k_D$  is not an adequate criterion for the existence of collective coordinates. Similar results to ours were found in this case by Rand<sup>17,18</sup> by considering individual particle trajectories in the self consistent field. This is simply a way of circumventing the use of

<sup>a</sup>Chapter 1 contained a covariant relativistic plasma response function formalism that was later incorporated into a paper on energy-momentum tensors for dispersive electromagnetic waves.<sup>15</sup>

the Vlasov equation but is equivalent to it. Rand makes an analogy between the symmetrical result of Pines and Bohm and the Gibbs paradox of fluid dynamics, and this analogy is upheld by the fact that Majumdar<sup>19,20</sup> and Cohen<sup>21</sup> get results in agreement with Pines and Bohm by using fluid dynamical treatments.

In this paper we consider a homogeneous isotropic magnetic-field-free plasma. We do not however restrict ourselves to a one-component plasma. In connection with the field around a small satellite, considered by Kraus and Watson,<sup>22</sup> it is necessary to consider the ions since the satellite velocity is comparable more with the ion velocity than the electron velocity. In this plasma there are two modes of longitudinal excitation, namely, ion acoustic waves and electron plasma waves, but if the test particle is much slower than the electron thermal velocity then only the ion waves can be excited—the case considered by the above authors. For ion waves not to be Landau damped out of existence the electron Debye length must be much greater than that of the ions, implying the electrons are much hotter than the ions or that the ions have a much greater charge. Kraus and Watson<sup>22</sup> also consider the case of a dense plasma, in which local thermal equilibrium may be assumed.

Despite the preceding remarks about two-component plasmas the case of infinite electron Debye length, which essentially reduces the problem to a one component model, has received the bulk of our attention. Most of our results therefore can only directly be compared with those of Majumdar.<sup>19,20</sup> We show that his neglect of Landau damping is not justified near the edge of the wake. The supersonic case receives brief attention in Sec. 3.3 and 3.5.

We note that Pappert<sup>23</sup> considered the effect of an ambient magnetic field on the wake of a test particle, but we do not treat this case. A considerable body of Russian work on the details of the satellite problem had also appeared by the time of this thesis.<sup>24,25,26,27</sup>

## 2. The Formal Solution

The electrostatic potential  $\varphi(\mathbf{x}, t)$  in the vicinity of a test particle of charge  $q$  moving rectilinearly at velocity  $\mathbf{v}_0$  ( $v_0 \ll c$ ) through a homogeneous, stable dispersive dielectric medium is obtained from standard linear response theory as

$$\varphi = \frac{q}{\varepsilon_0} \int \frac{d^3k}{(2\pi)^3} \frac{\exp[i\mathbf{k}\cdot(\mathbf{x} - \mathbf{v}_0 t)]}{k^2 \epsilon(\mathbf{k}\cdot\mathbf{v}_0, \mathbf{k})}. \quad (2.1)$$

(Henceforth we consider the time to be  $t = 0$ , when the test particle is at  $\mathbf{x} = 0$ , or, equivalently, represent the potential in a frame moving with the test particle.)

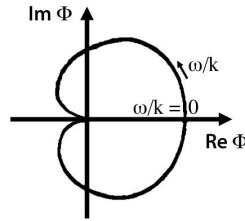


Fig. 1. The locus of  $\Phi(\omega/k)$  in the complex plane as the phase speed,  $\omega/k$ , is varied from  $-\infty$  to  $\infty$ . The point corresponding to  $\omega/k = 0$  is the intersection of the locus with the  $\text{Re}\Phi$  axis as indicated.

In Eq. (2.1)  $\epsilon(\mathbf{k}\cdot\mathbf{v}_0, \mathbf{k})$  is the *dielectric constant*, which, for an isotropic, collisionless unmagnetized plasma is given by

$$\epsilon(\omega, \mathbf{k}) \equiv \epsilon(\omega, |\mathbf{k}|) = 1 + \frac{\Phi(\omega/k)}{k^2}. \quad (2.2)$$

The function  $\Phi$  is defined by

$$\Phi(\omega/k) \equiv \sum_s \omega_{ps}^2 \int_{-\infty}^{\infty} dv \frac{g'_s(v)}{\omega/k - v + i0}, \quad (2.3)$$

$\omega_{ps}$  denoting the plasma frequency,  $(e_s^2 n_s / \epsilon_0 m_s)^{1/2}$  (SI units) for species  $s$ , with  $n_s$  the unperturbed number density,  $m_s$  the mass, and  $g_s(v)$  the one-dimensional projection of the unperturbed velocity distribution function  $f_s(\mathbf{v})$ . That is, in an arbitrary  $x, y, z$  Cartesian coordinate system,

$$g_s(v_z) \equiv \frac{1}{n_s} \iint dv_x dv_y f_s(\mathbf{v}), \quad (2.4)$$

the normalization factor  $1/n_s$  being introduced so that  $\int dv g_s \equiv 1$ . Henceforth we take  $s$  to denote electrons and a single species of ion, denoted by subscripts e and i respectively.

The assumed form of the “hodograph” of  $\Phi$  for each species is sketched in Fig. 1, which is such as to ensure stability towards exponentially growing oscillations by the Nyquist criterion [i.e. that the hodograph for  $\epsilon(\omega, k)$  not enclose the origin].

Equation (2.1) becomes now

$$\varphi = \frac{q}{\epsilon_0} \int \frac{d^3k}{(2\pi)^3} \frac{\exp(i\mathbf{k}\cdot\mathbf{x})}{k^2 + \Phi(\hat{\mathbf{k}}\cdot\mathbf{v}_0)}. \quad (2.5)$$

This is the starting point for all the following calculations. We shall consider only test particle velocities much less than the mean electron velocity so that we may approximate  $\Phi_e(\omega/k)$  to the static value  $k_{De}^2 \equiv \Phi_e(0)$ , the square of the (generalized) inverse Debye length for the electrons. Thus

$$\Phi(\omega/k) \approx k_{De}^2 + \omega_{pi}^2 \int_{-\infty}^{\infty} dv \frac{g'_i(v)}{\omega/k - v + i0}. \quad (2.6)$$

Note that if the electrons are extremely hot with respect to the ions then  $k_{De}^2 \rightarrow 0$  and the ions form an essentially one component plasma with the electrons forming a neutralizing background. The physical explanation of this is that, although the electrons are much lighter than the ions, they are moving too fast to be appreciably deflected from their paths within the range of the test particle and hence do not take part in the screening. If, on the other hand, the test particle has a velocity comparable with that of an average electron then the *ions* may be regarded as a uniform background due to their inertia. This case is therefore formally identical to the case  $k_{De}^2 = 0$ .

We give finally the normalized Maxwellian and Lorentzian distribution functions for a species  $s$  in a non-relativistic plasma together with the corresponding polarization functions  $\Phi_s$ .

*Maxwellian case:*

$$g_s(v) = \left( \frac{m_s}{2\pi T_s} \right)^{1/2} \exp -\frac{m_s v^2}{2T_s} = \frac{k_{Ds}}{(2\pi)^{1/2} \omega_{ps}} \exp -\frac{1}{2} \left( \frac{k_{Ds} v}{\omega_{ps}} \right)^2, \quad (2.7)$$

where  $m_s$  is the particle mass and  $T_s$  the temperature in energy units, giving

$$\begin{aligned} \Phi_s \left( \frac{\omega_{ps}}{k_{Ds}} x \right) &= k_{Ds}^2 \left[ 1 - \sqrt{2} x \exp \left( -\frac{x^2}{2} \right) \Psi \left( \frac{x}{\sqrt{2}} \right) \right. \\ &\quad \left. + i \left( \frac{\pi}{2} \right)^{1/2} x \exp \left( -\frac{x^2}{2} \right) \right], \end{aligned} \quad (2.8)$$

for any dimensionless  $x$ , where  $k_{Ds}^2 \equiv e_s^2 n_s / \epsilon_0 T_s$  and

$$\Psi(y) \equiv \int_0^y dt \exp t^2. \quad (2.9)$$

*Lorentzian case:*

$$g_s(v) = \frac{1}{\pi} \frac{u_{s0}}{v^2 + u_{s0}^2}. \quad (2.10)$$

$$\Phi_s \left( \frac{\omega_{ps}}{k_{Ds}} x \right) = \frac{k_{Ds}^2}{(1 - ix)^2}, \quad (2.11)$$

where  $k_{Ds} \equiv \omega_{ps}/u_{s0}$ .

### 3. Analytical approximations

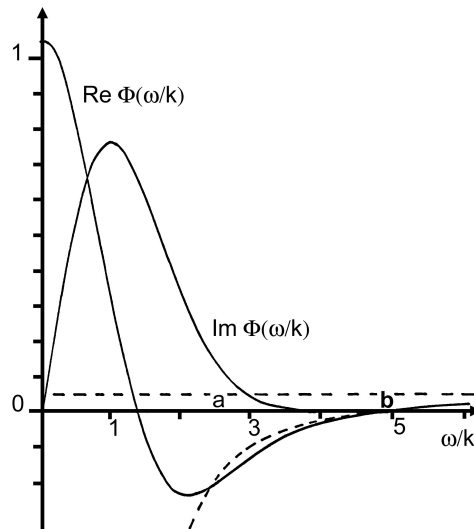


Fig. 2. The polarization function  $\Phi(\omega/k)$  (in units such that  $\omega_{pi} = k_{Di} = 1$ ) for a Maxwellian ion distribution and electron Debye constant  $k_{De}^2 = 0.5$  (dashed horizontal line). The asymptotic expansion  $k_{De}^2 - (k^2/\omega^2 + v_i^2 k^4/\omega^4)$  is included for comparison, being represented by the dashed curve.

Although it is clearly impossible analytically to evaluate the integral Eq. (2.5) for general  $g(v)$ , or even for as simple a distribution as the Lorentzian, one may derive approximations for the integral in various ranges of  $v_0$  that enable one to gain some understanding of its properties.

First we sketch  $\Phi(\omega/k)$  and its asymptotic expansion in Fig. 2.

#### 3.1. Small $v_0$

We note from equation Eq. (2.5) that the argument of  $\Phi \equiv \Phi_e + \Phi_i$  is less than or equal to  $v_0$ . Consequently for small  $v_0$  only the behaviour of  $\Phi$  near the origin will affect the potential.

Expanding about the origin,  $\Phi(w) = k_D^2 + ia_0w - a_1w^2 + O(w^3)$ , where  $a_0$  and  $a_1$  are positive constants depending on the distribution function, we get, in units such that  $k_D^2 \equiv k_{Di}^2 + k_{De}^2 = 1$ ,

$$\begin{aligned} \frac{1}{k^2 + \Phi(w)} &= \frac{1}{k^2 + 1} - \frac{ia_0w}{(k^2 + 1)^2} \\ &+ \left[ \frac{a_1}{(k^2 + 1)^2} - \frac{a_0^2}{(k^2 + 1)^3} \right] w^2 + \dots \end{aligned} \quad (3.1)$$

Then

$$\begin{aligned} \varphi(\mathbf{x}) &= \frac{q}{\varepsilon_0} \int \frac{d^3k}{(2\pi)^3} e^{i\mathbf{k}\cdot\mathbf{x}} \left\{ \frac{1}{k^2 + 1} - ia_0 \frac{\hat{\mathbf{k}}\cdot\mathbf{v}_0}{(k^2 + 1)^2} \right. \\ &\quad \left. + \left[ \frac{a_1}{(k^2 + 1)^2} - \frac{a_0^2}{(k^2 + 1)^3} \right] \mathbf{v}_0 \cdot \hat{\mathbf{k}} \hat{\mathbf{k}} \cdot \mathbf{v}_0 \right\} \\ &= \frac{q}{\varepsilon_0} \left\{ \frac{\exp(-r)}{4\pi r} - ia_0 \mathbf{v}_0 \cdot \hat{\mathbf{x}} \int \frac{d^3k}{(2\pi)^3} \frac{\hat{\mathbf{x}}\cdot\hat{\mathbf{k}}}{(k^2 + 1)^2} e^{i\mathbf{k}\cdot\mathbf{x}} \right. \\ &\quad \left. + \mathbf{v}_0 \mathbf{v}_0 : \left[ \int \frac{d^3k}{(2\pi)^3} \hat{\mathbf{k}} \hat{\mathbf{k}} e^{i\mathbf{k}\cdot\mathbf{x}} \left( \frac{a_1}{(k^2 + 1)^2} - \frac{a_0^2}{(k^2 + 1)^3} \right) \right] \right\} \end{aligned} \quad (3.2)$$

where  $\hat{\cdot}$  denotes a unit vector.

The first integral in the second line of Eq. (3.2) may be evaluated as follows

$$\begin{aligned} \int \frac{d^3k}{(2\pi)^3} \frac{\hat{\mathbf{x}}\cdot\hat{\mathbf{k}}}{(k^2 + 1)^2} e^{i\mathbf{k}\cdot\mathbf{x}} &= \frac{1}{(2\pi)^2} \int_{-1}^1 d\mu \int_0^\infty dk \frac{k^2}{(k^2 + 1)^2} e^{ik\mu r} \\ &= \frac{1}{i(2\pi)^2} \operatorname{Re} \frac{d}{dr} \left( \frac{1}{r} - \frac{d}{dr} \right) \eta(r), \end{aligned} \quad (3.3)$$

where  $\eta(r)$  is defined as follows

$$\eta(z) \equiv \frac{z}{i} \int_0^\infty dx \frac{\exp(ix)}{x^2 + z^2} \quad (3.4)$$

for  $|\arg z| < \pi/2$  and by analytic continuation elsewhere, cutting the complex plane along the negative imaginary axis. For details of the properties of  $\eta$  see Appendix I of the thesis.<sup>14</sup>

The tensor term in the second line of Eq. (3.2) may be evaluated by contour integration, yielding

$$\begin{aligned} \varphi(\mathbf{x}) &= \frac{q}{\varepsilon_0} \left\{ \frac{\exp(-r)}{4\pi r} - a_0 \frac{\hat{\mathbf{x}}\cdot\mathbf{v}_0}{(2\pi)^2} \operatorname{Re} \frac{d}{dr} \left( \frac{1}{r} - \frac{d}{dr} \right) \eta(r) \right. \\ &\quad \left. + \mathbf{v}_0 \cdot [\mathcal{T}_\parallel \hat{\mathbf{x}} \hat{\mathbf{x}} + \mathcal{T}_\perp (\mathbf{I} - \hat{\mathbf{x}} \hat{\mathbf{x}})] \cdot \mathbf{v}_0 \right\}, \end{aligned} \quad (3.5)$$

where

$$\mathcal{T}_{\parallel} \equiv \frac{1}{8\pi} \left\{ a_1 \left[ \left( 1 + \frac{2}{r} + \frac{4}{r^2} + \frac{4}{r^3} \right) e^{-r} - \frac{4}{r^3} \right] - \frac{a_0^2}{4} \left[ \left( r + 3 + \frac{8}{r} + \frac{16}{r^2} + \frac{16}{r^3} \right) e^{-r} - \frac{16}{r^3} \right] \right\}, \quad (3.6)$$

$$\mathcal{T}_{\perp} \equiv \frac{1}{8\pi} \left\{ a_1 \left[ \frac{2}{r^3} - \frac{1}{r} \left( 1 + \frac{2}{r} + \frac{2}{r^2} \right) e^{-r} \right] - \frac{a_0^2}{4} \left[ \frac{8}{r^3} - \left( 1 + \frac{4}{r} + \frac{8}{r^2} + \frac{8}{r^3} \right) e^{-r} \right] \right\}. \quad (3.7)$$

It is to be noted that, contrary to appearances,  $\mathcal{T}_{\parallel}$  and  $\mathcal{T}_{\perp}$  are regular at  $r = 0$ .

For large  $r$ , the asymptotic form of  $\eta(r) \sim 1/r$  holds and the exponential terms may be neglected. Thus, for  $r \rightarrow \infty$ ,

$$\varphi(\mathbf{x}) \sim \frac{q}{\varepsilon_0} \left\{ \frac{a_0}{\pi^2} \frac{\hat{\mathbf{x}} \cdot \mathbf{v}_0}{r^3} + \frac{(a_0^2 - a_1)}{2\pi} \frac{(\hat{\mathbf{x}} \cdot \mathbf{v}_0)^2}{r^3} - \frac{(a_0^2 - a_1)v_0^2}{4\pi} \frac{[1 - (\hat{\mathbf{x}} \cdot \hat{\mathbf{v}}_0)^2]}{r^3} \right\}. \quad (3.8)$$

The first term is dominant for  $|\hat{\mathbf{x}} \cdot \mathbf{v}_0| \gg 0$  i.e. for all directions not oblique to the direction of motion. The field is reminiscent of a dipole field except that it decays more rapidly with  $r$ . This may qualitatively be interpreted as meaning that the centre of the screening cloud has been displaced to a position behind the particle. It is this asymmetry that gives rise to the drag on a very heavy particle moving at subthermal speeds and, since this drag is the summation of the field of each individual particle moving in the average field of all the others, one supposes that the drag thus calculated includes single particle effects to the extent of validity of the linearized theory,<sup>b</sup> i.e. except for very close collisions.

Rand<sup>17</sup> has calculated the screened field to first order in  $v_0$  by considering the trajectories of individual particles, explicitly rather than through the Vlasov equation. He obtains a function  $\phi_1(x)$  as a triple integral, which he apparently evaluates numerically but which agrees exactly<sup>c</sup> with values calculated from  $\frac{1}{2}\text{Re}(d/dx)(d/dx - 1/x)\eta(x)$ .

<sup>b</sup>This is confirmed by the work of Hubbard<sup>11</sup> who shows that the friction coefficient is the sum of the ‘‘self field’’ term and a fluctuating microfield term which vanishes in the limit of infinite test-particle mass, as do the higher transition moments.

<sup>c</sup>There is an error in Eq. (26) of Ref. 2, namely that the second  $Z$  in the equation should be replaced by  $2Z/(Z+1)$ .



It is interesting to note that the solution we have obtained differs completely from that of Pines and Bohm<sup>16</sup> and workers who have used linearized fluid dynamical equations.<sup>19,21</sup> We ascribe this discrepancy to these authors' use of a collective approach in a region in which it is not valid: Inspection of Fig. 2 shows that the region in which collective coordinates exist can only be  $|\omega/k| \gtrsim \bar{v}_i^2$ , which is never entered in the case of a slow particle. The criterion  $k \lesssim k_{Di}$  is not adequate in the case of forced oscillations since  $\omega$  may be much less than  $\omega_{pi}$ .

We note that behind the test particle the potential has opposite sign to its unscreened value, which we refer to as positive. At right angles to the direction of motion the first order term vanishes and the second-order term dominates. We see that  $\varphi(\mathbf{x})$  goes negative in this direction if  $a_0^2 > a_1$ . For the Lorentzian distribution we have from Eq. (2.11)  $\Phi_i(x) = 1 + 2ix - 3x^2 + k_{De}^2 + O(x^3)$ , in units where  $\omega_{pi} = k_{Di} = 1$ . Thus  $a_0 = 2$  and  $a_1 = 3$ , and therefore  $a_0^2 > a_1$  so that the  $90^\circ$  potential does go negative somewhere between  $r = 0$  and  $r = \infty$ .

We shall now discuss the situation when the particle has sufficient velocity for wave excitation to be possible.

The dispersion relation for plasma waves is  $\epsilon(\omega, k) = 0$ , i.e.

$$\Phi(\omega/k) = -k^2, \quad (3.9)$$

where  $\omega$  is in general complex, but if the waves are but slightly damped then we may take  $\omega$  real as a first approximation. It is then clear that only the regions in which  $\text{Re}\Phi(\omega/k)$  is negative are available for excitation. In Fig. 2 this means the region  $a < \omega/k < b$  which, it will be noted, exists if  $k_{De}^2$  is sufficiently small.

This is the region of ion acoustic waves, which resemble sound waves in ordinary gases in that there is an upper bound,  $b$ , to their phase velocity. To guide our mathematical investigations we shall endeavour to give a physical picture of the processes that can occur.

If a particle has a velocity  $v_0$ ,  $a < v_0 < b$ , then it can excite waves with the same phase velocity as its own velocity. We might therefore expect it to be followed by a train of waves with this phase velocity, spreading out laterally with the maximum group velocity possible. This is roughly indicated in Fig. 3.

If  $v > b$  then we can expect no monochromatic train but some kind of shock wave confined within the "Mach cone". This is analogous to the formation of the shock wave behind a supersonic object in the atmosphere or to a longitudinal Cerenkov radiation.

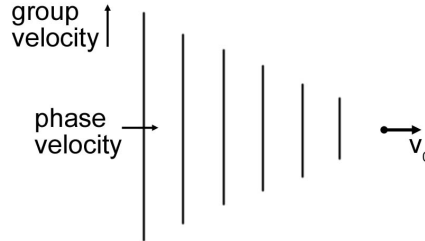


Fig. 3. Schematic of wake field behind a charged test particle moving through a plasma.

A note of caution must be sounded at this point with respect to the spreading out of the wake. Since this is controlled by the interference of the generated waves it is critically dependent on the dispersive nature of the medium, as will be discussed later. It is well known that in regions of anomalous dispersion in optical media the concept of group velocity breaks down entirely.<sup>28</sup> We thus expect the situation to be complicated if Landau damping becomes important.

Since we are seeking wave behaviour a contour integral method is the obvious choice and has been much used, see e.g. Ref. 16. We indicate the general method below as well as some of its analytical difficulties, not mentioned in the literature due in effect to the assumption from the outset that an asymptotic form for the dielectric constant is a valid approximation.

In equation Eq. (2.5) use cylindrical coordinates with axis parallel to  $\mathbf{v}_0$ . Then

$$\varphi = \frac{q}{(2\pi)^2 \epsilon_0} \int_0^\infty dk_\perp k_\perp J_0(k_\perp x_\perp) \times \int_{-\infty}^\infty dk_1 \exp(ik_1 x_1) \left[ k_1^2 + k_\perp^2 + \Phi \left( \frac{k_1 v_0}{(k_1^2 + k_\perp^2)^{1/2}} \right) \right]^{-1}. \quad (3.10)$$

The contour in the  $k_1$  integral may be completed in the lower/upper half of the complex  $k_1$  plane according as  $x_1 \leq 0$ . However, note that, since  $k_1 = \pm k_\perp$  are branch points, the contours must be indented as shown in Fig. 4. The zeros of the denominator will give rise to poles whose contributions may be evaluated by the method of residues.

For reasonably stable distributions, at least, one may show that the plasma wave poles corresponding to Eq. (3.9) are in the lower half  $k_1$  plane. Consequently there is a wave excitation only *behind* the particle. There are

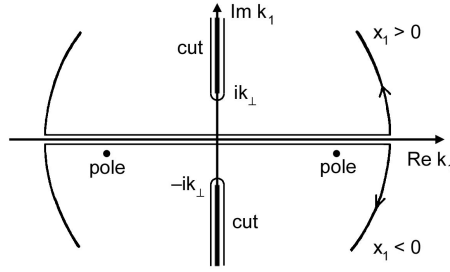


Fig. 4. Contours used in the evaluation of the  $k_1$  integral in Eq. (3.10).

other zeros of  $\epsilon$  somewhere in the lower half plane, but since they give rise to strongly damped contributions, one hopes that they may be ignored, at any rate for large  $|x_1|$ . Indeed the contribution from the region of the cut will also be negligible compared with the wave contribution.

For  $x_1 > 0$  it is necessary to consider the contribution from the region of the cut. The part nearest the real axis is clearly the most important for large  $|x_1|$ , so let us consider the region around  $ik_\perp$

In this region  $|k_1 v_0 / (k_1^2 + k_\perp^2)^{1/2}|$  is large and the asymptotic expansion for  $\Phi$  may be used. This may be obtained from Eq. (2.6) by expanding the denominator and integrating term by term.

$$\Phi(z) = k_{De}^2 - \omega_{pi}^2 \left( \frac{1}{z^2} + \frac{\overline{v_1^2}}{z^4} \right) - 2\pi i \theta(-\text{Im}z) g_1'(z) \omega_{pi}^2, \quad (3.11)$$

where the last term is required for analytical continuation into the lower half  $z$  plane. Here  $\overline{v_1^2}$  is the mean-square ion speed (the square of the *ion thermal speed* in a Maxwellian plasma). However, if  $k_1$  is in the lower/upper half plane, so also is  $k_1 / (k_1^2 + k_\perp^2)^{1/2}$ . Hence the analytical continuation term is not required in the region we are considering. At  $k_1 = -ik_\perp$  it gives rise in general to an essential singularity, but this contribution is being neglected as mentioned above. We now note the curious fact that the asymptotic expansion is single-valued in the upper half plane since only even powers of  $(k_1^2 + k_\perp^2)^{1/2}$  occur. Thus there is only a simple pole in the neighbourhood of  $k_1 = ik_\perp$ .

For simplicity let us retain only terms to order  $1/z^2$ . Note that to this order the maximum phase velocity is

$$b = \omega_{pi} / k_{De} \equiv C_s, \quad (3.12)$$

the constant  $C_s$  being commonly called the *ion sound speed*.

### 3.2. Intermediate velocity $(\bar{v}_1^2)^{1/2} \ll v_0 < C_s$ (forward field)

If  $v_0 \ll b$  then the pole is approximately at  $k_1 = ik_\perp$  and we may take  $k_{De} = 0$  without greatly altering the situation. Then

$$\varphi = \frac{q}{4\pi\epsilon_0} \left[ \frac{1}{r} - \frac{\omega_{pi}}{v_0} \int_0^\infty dy \frac{J_0(\omega_{pi}x_\perp y/v_0) \exp(-\omega_{pi}x_1 y/v_0)}{1+y^2} \right]. \quad (3.13)$$

An alternative form is obtained by noting that<sup>29</sup>

$$\begin{aligned} \frac{1}{r} &= \int_0^\infty dk_\perp J_0(k_\perp x_\perp) \exp(-x_1 k_\perp) \\ &= \frac{\omega_{pi}}{v_0} \int_0^\infty dy J_0\left(\frac{\omega_{pi}x_\perp y}{v_0}\right) \exp\left(-\frac{\omega_{pi}x_1 y}{v_0}\right). \end{aligned} \quad (3.14)$$

Thus

$$\varphi = \frac{q}{4\pi\epsilon_0} \frac{\omega_{pi}}{v_0} \int_0^\infty dy \frac{y^2}{1+y^2} J_0\left(\frac{\omega_{pi}x_\perp y}{v_0}\right) \exp\left(-\frac{\omega_{pi}x_1 y}{v_0}\right). \quad (3.15)$$

Note that the characteristic length is now  $v_0/\omega_{pi}$ , the distance the particle moves in an ion plasma oscillation time, rather than the ion Debye length. The new length is longer, and furthermore, the screening is again not exponential at large  $r$  as we shall now show.

$$\begin{aligned} \text{For } x_\perp = 0: \varphi &= \frac{q}{4\pi\epsilon_0} \frac{1}{x_1} \left[ 1 - \frac{\omega_{pi}x_1}{v_0} i\eta \left( \frac{i\omega_{pi}x_1}{v_0} \right) \right] \\ &\sim \frac{q}{4\pi\epsilon_0} \frac{2\omega_{pi}}{v_0} \left( \frac{\omega_{pi}r}{v_0} \right)^{-3}. \end{aligned} \quad (3.16)$$

$$\begin{aligned} \text{For } x_1 = 0: \varphi &= \frac{q}{4\pi\epsilon_0} \frac{1}{x_\perp} \left\{ 1 - \frac{\omega_{pi}x_\perp}{v_0} \left[ I_0\left(\frac{\omega_{pi}x_\perp}{v_0}\right) - \mathbf{L}_0\left(\frac{\omega_{pi}x_\perp}{v_0}\right) \right] \right\} \\ &\sim -\frac{q}{4\pi\epsilon_0} \frac{\omega_{pi}}{v_0} \left( \frac{\omega_{pi}r}{v_0} \right)^{-3}, \end{aligned} \quad (3.17)$$

where  $I_0$  and  $\mathbf{L}_0$  modified Bessel and Struve functions respectively.

A general asymptotic form at large  $r$  may be obtained from Eq. (3.15) by approximating the denominator to 1 and differentiating Eq. (3.14) twice with respect to  $\omega_{pi}x_1/v_0$ . Thus

$$\varphi \sim \frac{q}{4\pi\epsilon_0} \frac{\omega_{pi}}{v_0} \frac{2(\hat{\mathbf{x}} \cdot \hat{\mathbf{v}}_0)^2 - (\hat{\mathbf{x}} \times \hat{\mathbf{v}}_0)^2}{(\omega_{pi}r/v_0)^3} \quad (3.18)$$

Note that this obeys the same inverse third power law as in the very low velocity case, and also as in this case the field goes negative, for large  $r$ , at large angles between  $\hat{\mathbf{x}}$  and  $\hat{\mathbf{v}}_0$ . The angle at which the field changes sign is approximately  $55^\circ$ .

### 3.3. Supersonic velocities $v_0 > C_s$ (forward field)

As  $v_0$  increases beyond maximum phase velocity  $b$  (the ion sound speed) the pole moves from  $ik_\perp$  to  $ik_{De}$  and the forward field changes to a Debye potential with Debye length  $k_{De}^{-1}$ . This has the physical interpretation that if the particle velocity greatly exceeds the maximum ion wave phase velocity then the ions are too sluggish to participate in the screening.

We must now discuss the case  $x_1 < 0$  where plasma wave excitation is assumed to be the dominant contribution. The positions of the plasma wave poles are given by the dispersion relation Eq. (3.9). It will be assumed that the asymptotic expansion Eq. (3.11) represents a valid approximation to  $\Phi$ , with the one alteration that, since  $z$  is on or near the real axis, the last term is  $-i\pi g'_i(z)$ . [It will be noted that in a sector containing the real axis  $g'_i(z)$  usually decays exponentially, and the factor multiplying it is irrelevant to the *asymptotic expansion*; but we require an *approximation* to  $\Phi$  and so analytically continue off the real axis where the  $i\pi$  factor is known to be exact.]

The dispersion relation is now

$$k^2 + k_{De}^2 - \omega_{pi}^2 \left( \frac{k^2}{\omega^2} + \overline{v_i^2} \frac{k^4}{\omega^4} \right) - i\pi \omega_{pi}^2 g'_i \left( \frac{\omega}{k} \right) = 0. \quad (3.19)$$

This is valid for  $|\omega/k| \gg (\overline{v_i^2})^{1/2}$ , i.e. when the “finite temperature” term  $v_i^2 k^4 / \omega^4$  is small compared with  $k^2 / \omega^2$ .

### 3.4. Intermediate velocity $(\overline{v_i^2})^{1/2} < v_0 < C_s$ (wake)

We again make the simplifying assumption that  $k_{De} = 0$ . The dispersion relation can now be reduced to the familiar form

$$\omega^2 \approx \omega_{pi}^2 + \overline{v_i^2} k^2 + i\pi \omega_{pi}^2 \operatorname{sgn} \omega \left( \frac{\omega_{pi}}{k} \right)^2 g'_i \left( \frac{\omega_{pi}}{k} \right) = 0. \quad (3.20)$$

To simplify the analysis let us use units such that  $k_{Di} = \omega_{pi} = 1$ . In these units  $\overline{v_i^2} = 3$  (Maxwellian case), and generally we may assume  $\overline{v_i^2} \sim 1$ .

The finite temperature correction is small provided  $k^2 \ll 1$ , i.e. for wavelengths much greater than a Debye length. Thus, for the dispersion

relation to be valid, we must require both  $|k_1| \ll 1$  and  $k_\perp \ll 1$ . Since  $\omega = k_1 v_0 \approx 1$  it is clear that we require  $v_0 \gg 1$ .

Substituting  $\omega = k_1 v_0$  and  $k^2 = k_1^2 + k_\perp^2$ , and assuming  $k_\perp$  small, we find

$$k_1 = \pm \frac{1}{v_0} \left\{ 1 + \frac{\alpha}{2} + \alpha v_0^2 k_\perp^2 \pm \frac{i\pi}{2} \left[ \frac{1+\alpha}{v_0^2} + k_\perp^2 \right]^{-1} g' \left( \left[ \frac{1+\alpha}{v_0^2} + k_\perp^2 \right]^{-1/2} \right) \right\}, \quad (3.21)$$

where  $\alpha \equiv v_i^2/v_0^2 \ll 1$ .

The last term takes account of Landau damping and,  $g'(v)$  being negative, serves to displace the poles in Fig. 4 below the real  $k_1$  axis. Neglecting the damping term, which is very small until  $k_\perp$  gets close to 1, we find

$$\begin{aligned} \frac{\partial}{\partial k_1} \left[ k_1^2 + k_\perp^2 + \Phi \left( \frac{k_1 v}{(k_\perp^2 + k_1^2)^{1/2}} \right) \right]_{\text{poles}} \\ = \pm \frac{2}{v} \left( 1 + \frac{\alpha}{2} \right) \left( 1 + \frac{\alpha}{2} y^2 \right) (1 + y^2), \quad (3.22) \end{aligned}$$

where  $y \equiv k_\perp v_0$ .

The two factors containing  $\alpha$  are small correction terms. Using Eq. (3.21) to locate the poles and Eq. (3.22) to evaluate the residues we find from Eq. (3.10) that

$$\varphi = \frac{2-\alpha}{v_0} \text{Im} \left[ \exp \left( -i \left[ 1 + \frac{\alpha}{2} \right] \left| \frac{x_1}{v_0} \right| \right) I \left( \frac{\alpha}{2} \left| \frac{x_1}{v_0} \right|, \frac{x_\perp}{v_0}, \frac{\alpha}{2} \right) \right], \quad (3.23)$$

where

$$\gamma(y) \equiv -\frac{\pi}{2} \frac{v_0^2}{(1+\alpha+y^2)} g' \left( \frac{v_0}{(1+\alpha+y^2)^{1/2}} \right) \quad (3.24)$$

is the Landau damping term, which has the effect of rapidly cutting off the integral when  $|y|$  gets close to  $v_0$ , and  $I$  is the integral

$$I(a, b, c) \equiv \int_0^\infty dy y \frac{J_0(by) \exp(-iay^2)}{(1+y^2)(1+cy^2)} \psi(y), \quad (3.25)$$

with

$$\psi(y) \equiv \exp \left( - \left| \frac{x_1}{v_0} \right| \gamma(y) \right). \quad (3.26)$$

In Eq. (3.23) the substitutions for the dummy arguments  $a$ ,  $b$  and  $c$  are

$$a = \frac{\alpha}{2} \left| \frac{x_1}{v_0} \right|, \quad b = \frac{x_\perp}{v_0} \quad \text{and} \quad c = \frac{\alpha}{2}. \quad (3.27)$$

When  $b = 0$  we suppose that the cutoff factor  $\psi$  may be neglected. Then

$$I(a, 0, c) \approx \frac{1}{2(1-c)} \left[ e^{ia} E_1(ia) - e^{ia/c} E_1\left(\frac{ia}{c}\right) \right] \quad (3.28)$$

where  $E_1$  is the exponential integral.<sup>30</sup>

To obtain an asymptotic form in the general case it is helpful to transform the one-sided integral into a two-sided integral by a method due to Hankel,<sup>29</sup> noting that, for  $x > 0$ ,

$$J_0(x) = \frac{1}{2} \left[ H_0^{(1)}(x) - H_0^{(1)}(-x + i0) \right], \quad (3.29)$$

where  $H_0^{(1)}(z)$  is a Hankel function, defined on the complex  $z$ -plane cut along the negative real axis, being regular elsewhere. Then

$$I(a, b, c) = \frac{1}{2} \int_{-\infty}^{\infty} dy y \frac{H_0^{(1)}(b[y + i0]) \exp(-ia y^2)}{(1 + y^2)(1 + cy^2)} \psi(y). \quad (3.30)$$

If  $a$  were zero and  $\psi$  well behaved, we could evaluate the integral by completing the contour in the upper half plane. Instead we seek the saddle points and poles of the integrand, the poles being at  $y = \pm i$  and  $y = \pm i/\sqrt{c}$ . To find the saddle points let us suppose that the asymptotic form for  $H_0^{(1)}(z)$ ,

$$H_0^{(1)}(z) \sim \sqrt{\frac{2}{\pi}} \frac{\exp i(z - \frac{\pi}{4})}{\sqrt{z}}, \quad |z| \rightarrow 0, \quad (3.31)$$

is valid in the region of these points. (The asymptotic form will be valid in the region of the poles provided  $|b| \gg 1$ ,  $c < 1$ .)

Since the denominator is slowly varying away from its zeros the saddle points are determined by the exponential factor, the exponent of which, being quadratic, has only one stationary point. This is at  $y = y_0$ , where  $y_0 = b/2a$ . For Eq. (3.30) to be valid we require  $|y_0| \gg 1$ .

We conclude that, provided the two conditions  $b \gg 1$  and  $b \gg 2|a|$  are satisfied, we may approximate  $I$  by

$$I(a, b, c) \approx \frac{e^{-i\pi/4}}{\sqrt{b}} \sqrt{2\pi} \int_{-\infty}^{\infty} \frac{dy}{2\pi} \frac{(y + i0)^{1/2} \exp(-ia y^2) \psi(y)}{(1 + y^2)(1 + cy^2)} e^{iby}. \quad (3.32)$$

This is a Fourier transform, which may be transformed by the convolution theorem to

$$I(a, b, c) \approx \frac{e^{-i\pi/4}}{\sqrt{b}} \frac{1}{\sqrt{2\pi}} \psi_b * \int_{-\infty}^{\infty} dy \frac{(y + i0)^{1/2} \exp(-ia y^2) e^{iby}}{(1 + y^2)(1 + cy^2)}, \quad (3.33)$$

where  $\psi_b \equiv \int_{-\infty}^{\infty} \psi(y) e^{iby} dy / 2\pi$  is a delta-like function of  $b$  with width  $1/v_0$ , which will have the effect of destroying all wave structure with wavelength of a Debye length or less.

The integral may now be estimated by deforming the contour of integration to cross the saddle point along the line of steepest descent. (The pole at  $i/\sqrt{c}$ , being far up the imaginary axis, gives negligible contribution.)

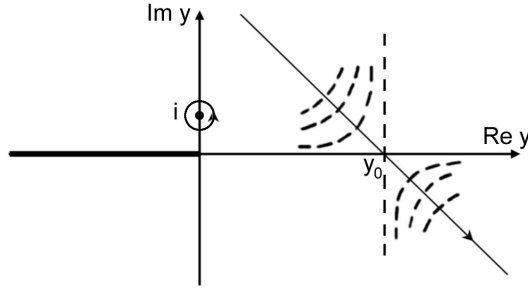


Fig. 5. The contour used for estimating the integral in Eq. (3.33).

We make the further requirement that the width of the saddle at  $y_0$  be much less than  $y_0$ . That is,  $1/\sqrt{a} \ll y_0$ . Then

$$I(a, b, c) \approx \psi_b * \left[ \sqrt{\frac{\pi}{2b}} \frac{e^{ia-b}}{1-c} - \frac{i}{\sqrt{2ab}} \frac{y_0^{1/2} \exp(ib^2/4a)}{(1+y_0^2)(1+cy_0^2)} \right]. \quad (3.34)$$

Since the first term varies slowly compared with  $\psi_b$ , the convolution will leave it but little changed, whereas the rapid fluctuations in  $\exp(ib^2/4a)$  will be damped out. Supposing that the exponential term may locally be approximated by a monochromatic wave, we finally obtain

$$I(a, b, c) \approx \sqrt{\frac{\pi}{2b}} \frac{e^{ia-b}}{1-c} - \frac{i}{\sqrt{2ab}} \frac{y_0^{1/2} \exp(ib^2/4a)}{(1+y_0^2)(1+cy_0^2)}, \quad (3.35)$$

with  $y_0 = b/2a$ .

The method of steepest descent we have used to approximate the integral is equivalent, in the neighbourhood of the saddle point, to the method of stationary phase employed by Majumdar<sup>20</sup> but takes better account of the behaviour away from the saddle point by including the contribution of the pole at  $y = i$ . We have also attempted to take some account of Landau damping, which the above author was unable to do owing to his formulation in terms of fluid dynamics.



Below we recapitulate the criteria for the validity of Eq. (3.35)

$$c \ll 1, \quad b \gg 1, \quad b \gg 2a, \quad b \gg 2\sqrt{a}. \quad (3.36)$$

With  $a$ ,  $b$  and  $c$  given by Eq. (3.27) these correspond physically (recalling that in this subsection we are using units such that  $k_{Di} = \omega_{pi} = 1$ ) to the inequalities

$$\frac{\alpha}{2} \ll 1, \quad \frac{x_{\perp}}{v_0} \gg 1, \quad x_{\perp} \gg \alpha|x_1|, \quad x_{\perp} \gg (\overline{v_i^2}|x_1|)^{1/2}. \quad (3.37)$$

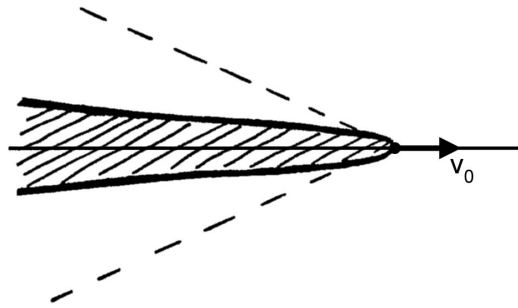


Fig. 6. Schematic of the wake region of an intermediate-velocity test particle indicating where the approximations used to derive Eq. (3.35) break down (hatched region) and the “thermal Mach cone” (dashed line).

Observe that the Landau damping term cuts off the second term at about  $x_{\perp} = |x_1|/v_0$ , which might be called a thermal Mach cone. This behaviour can be understood from the fact that plasma waves with high group velocity have low phase velocity, and hence are strongly damped. The first term, however, is unaffected by Landau damping and exhibits no thermal Mach cone, although it decays exponentially with  $x_{\perp}$ . We indicate the thermal Mach cone and the region excluded by the inequalities in Eq. (3.37) in Fig. 6.

### 3.5. Supersonic velocities $v_0 > C_s$ (wake field)

This is the case considered by Kraus and Watson<sup>22</sup> but their treatment neglects finite ion temperature effects on the dispersion relation and is consequently inadequate for finding variations over distances less than  $k_{De}^{-1}$ . We shall not go into detail on this case but shall indicate the approximations that may be made and the integral obtained.

The simplifying assumption made by the above authors can be represented as

$$(\overline{v_i^2})^{1/2} \ll b \ll v_0, \quad (3.38)$$

where  $b$  is here the upper bound to the phase velocity [ $\approx C_s$  by Eq. (3.12)], not the dummy argument used in the previous subsection. Taking units such that  $\omega_{pi} = k_{De} = 1$  we have

$$\overline{v_i^2} \ll 1, \quad b \approx 1, \quad v_0 \gg 1 \quad \text{and} \quad k_{Di} \gg 1. \quad (3.39)$$

Using the same methods as before, but neglecting Landau damping, we find the approximate form for  $x_1 < 0$

$$\varphi \approx -\frac{2}{v_0} \int_0^\infty \frac{dk_\perp k_\perp^2}{(1+k_\perp^2)^{3/2}} J_0(x_\perp k_\perp) \sin\left(\left|\frac{x_1}{v_0}\right| \frac{k_\perp(1+\frac{1}{2}\overline{v_i^2}k_\perp^2)}{(1+k_\perp^2)^{1/2}}\right). \quad (3.40)$$

Kraus and Watson in effect assume that the critical part of the integral for determining the large  $|x_1|/v_0$  behaviour of ( $x_\perp$  small) is near  $k_\perp = 0$  so that terms such as  $1+k_\perp^2$  may be approximated to 1. However, it must be observed that there is a range of  $k_\perp$  (between 1 and  $1/\overline{v_i^2}$ ) in which the argument of the sine function is but slowly varying. This suggests that, superimposed on the endpoint contribution, there may be a sinusoidal term.

When  $x_\perp$  is not small we may transform the integral into a two-sided integral as in Sec. 3.4. There will be a saddle point which disappears into the origin at the Mach cone  $x_\perp = |x_1|/v_0$ , but the contribution from the singularities of the integrand will be complicated by the essential singularities at  $k_\perp = \pm i$ .

#### 4. Numerical Solution

The explorations of the previous section showed that some insight into the nature of the fields around a particle in a collisionless plasma, as given formally by Eq. (2.1), may be obtained by asymptotic analyses in various limits. However, these are often difficult and the errors difficult to quantify. It is thus essential to supplement such analytic work with numerical and graphical methods (and *vice versa*).

In this section we summarize how this was done computationally in my MSc thesis work<sup>14</sup> using the newly arrived IBM 7044 (which had just replaced the Australian-built computer CSIRAC<sup>31</sup>).

#### 4.1. Formulation of the numerical method

To evaluate the integral Eq. (2.1) numerically we must choose axes such that as much of the integration as possible may be done analytically while the remaining integrations are as tractable as possible. It is found that, although one may come tantalizingly close to reducing the triple integral to a single integral, it is in general necessary to evaluate a double integral.

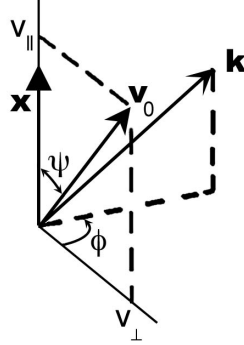


Fig. 7. Coordinate system used for numerical evaluation of the triple integral in Eq. (2.1).

Three systems of coordinates suggest themselves: the cylindrical coordinates of Sec. 3, spherical polars with axis along  $\mathbf{v}_0$ , and spherical polars with axis along  $\mathbf{x}$ . The first method involves infinite integrals with integrands having a large peak near the plasma wave pole and we consequently reject it. The last choice appears to have the advantage over the remaining one that it is easier to understand the behaviour of the integrands (at least at low  $\mathbf{v}_0$ ) and to isolate the singularity caused by the behaviour of  $\eta(x)$  at  $x = 0$ . These axes are sketched in Fig. 7. In this coordinate system we have

$$\hat{\mathbf{k}} \cdot \mathbf{v}_0 = \mu v_{\parallel} + \sqrt{1 - \mu^2} \cos \phi v_{\perp}, \quad (4.1)$$

where  $v_{\parallel} \equiv \mathbf{v}_0 \cdot \hat{\mathbf{x}} = v_0 \cos \psi$ ,  $v_{\perp} \equiv |\mathbf{v}_0 \times \hat{\mathbf{x}}| = v_0 \sin \psi$ , and  $\mu \equiv \hat{\mathbf{k}} \cdot \hat{\mathbf{x}}$ .

In these coordinates Eq. (2.1) becomes

$$\varphi = \frac{q}{(2\pi)^3 \varepsilon_0} \int_{-1}^1 d\mu \int_0^{2\pi} d\phi \operatorname{Re} \int_0^{\infty} dk \frac{k^2 \exp(ik\mu r)}{k^2 + \Phi(\mu v_{\parallel} + \sqrt{1 - \mu^2} \cos \phi v_{\perp})}, \quad (4.2)$$

where  $r \equiv |\mathbf{x}|$  and  $\Phi$  is defined in Eq. (2.3). The units used were such that  $k_{\text{Di}} = \omega_{\text{pi}} = 1$  and  $q = 4\pi\varepsilon_0$ .

By using the fact that  $\Phi(x)^* = \Phi(-x)$  for real  $x$ , the range of the  $\mu$  and  $\phi$  integrations was reduced by half. It was found useful<sup>14</sup> to define the new special function  $\eta(z)$ , Eq. (3.4). Analytical properties of  $\eta(z)$  are discussed in Appendix I of the thesis<sup>14</sup> and a listing of a Fortran IV subroutine for its efficient evaluation is given. This was used in the code developed to calculate the results presented below. (More discussion of the numerical method is given in the thesis.<sup>14</sup>)

In terms of  $\eta$ , Eq. (4.2) reduces to a double integration

$$\varphi = \frac{2}{\pi^2 r} \int_0^\pi d\phi \left\{ \frac{\pi}{2} + \int_0^r dx \operatorname{Im} \left[ \sqrt{\Phi} \eta(x\sqrt{\Phi}) \right] \right\}, \quad (4.3)$$

where

$$\sqrt{\Phi} \equiv \left\{ \Phi \left( \frac{xv_{\parallel}}{r} + \left[ 1 - \left( \frac{x}{r} \right)^2 \right]^{1/2} \cos \phi v_{\perp} \right) \right\}^{1/2}. \quad (4.4)$$

#### 4.2. Small $v_0$ results

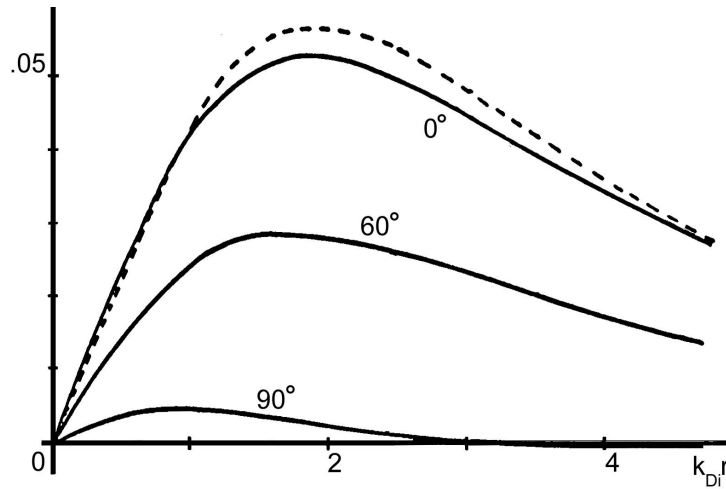


Fig. 8. Solid curves are the computed deviation from the Debye potential, as defined in the text, for a particle moving at velocity  $v_0 = 0.2\omega_{pi}/k_{Di}$  through a plasma with Lorentzian ion distribution and infinite-temperature electrons. Dashed curve is an analytic approximation to the forward field from Eq. (3.5).

The case where the test particle is travelling slower than the ion thermal speed was studied using the Lorentzian distribution function Eq. (2.10) with

$k_{De} = 0$ . The treatment of Sec. 3.1 indicates that the choice of distribution function and electron Debye length simply alters the relative magnitude of the constants  $k_D$ ,  $a_0$  and  $a_1$ , so we expect there is little to be gained by study of a large variety of cases.

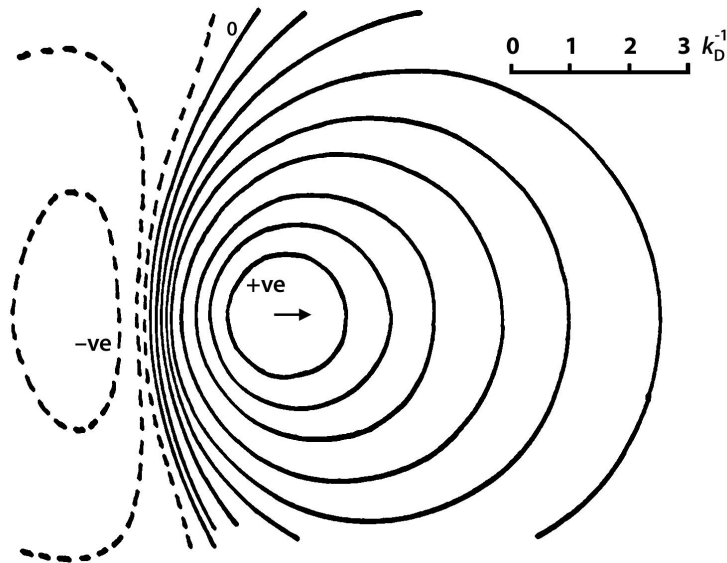


Fig. 9. Equipotentials in a plasma the same as assumed for Fig. 8 but with  $v_0 = 0.4\omega_{pi}/k_{Di}$  (the direction of  $\mathbf{v}_0$  is indicated by an arrow). The solid equipotentials indicate positive (+ve)  $\varphi$  and the dashed lines negative (-ve). The scale in Debye lengths is indicated top right.

In Fig. 8 we plot the deviation from the Debye potential along lines making angles  $\psi$  of  $0^\circ$ ,  $60^\circ$  and  $90^\circ$  to the direction of travel, the deviation being defined as  $[\varphi(\mathbf{x}) - \varphi_D(r)]/\varphi_0(r)$ , where  $\varphi_D(r) \equiv q \exp(-k_{Di}r)/4\pi\epsilon_0 r$  is the Debye potential and  $\varphi_0(r) \equiv q/4\pi\epsilon_0 r$  is the bare, unscreened potential. The approximate result at  $0^\circ$  obtained from the term of Eq. (3.5) first order in  $v_0$  is also plotted (dashed curve), the agreement being seen to be quite reasonable.

The qualitative form of Fig. 9 is also in agreement with that predicted from the analytical work. Note the potential well behind the particle, beyond which the field becomes attractive to charges of the same sign as the test particle.

### 4.3. Intermediate $v_0$ results

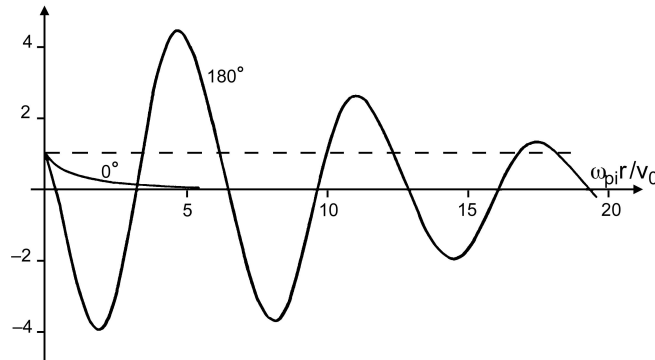


Fig. 10. Plots of  $\varphi(r, \psi)/\varphi_0(r)$  as a function of distance  $r$  (in units of  $v_0/\omega_{pi}$ ) calculated for a test particle moving at  $v_0 = 8\omega_{pi}/k_{Di}$  in a plasma with Lorentzian ions and  $k_{De} = 0$ . The forward field is labelled  $0^\circ$  and the wake field is labelled  $180^\circ$ . The dashed line is the unscreened case,  $\varphi = \varphi_0$ .

The intermediate case, where the test particle moves faster than the ion thermal speed but less than the ion sound speed  $C_s$ , was studied in part using both Lorentzian and Maxwellian distribution functions as these to some extent represent extremes of Landau damping. The Lorentzian distribution is sufficiently simple for an exact dispersion relation to be derivable, thus obviating the use of asymptotic expansions of  $\Phi$ . Again we took  $k_{De} = 0$ , so  $C_s = \infty$  by Eq. (3.12).

Potentials on the axis of symmetry, parallel (forward field,  $\psi = 0$ ) or antiparallel (wake field,  $\psi = \pi$ ) to the direction of motion of the test particle, are plotted in Figs. 10–12:

*Forward field:* In all three of the plots the results agreed well with Eq. (3.16), with agreement particularly good for the Maxwellian case (four significant figures at  $v_0 = 8\omega_{pi}/k_{Di}$ . [The potentials at  $90^\circ$  to the direction of motion also agreed reasonably with Eq. (3.17).]

*Wake field, Lorentzian case, Fig. 10:* Within the wake Landau damping had a dominant effect in the Lorentzian case even at the centre of the wake. This is due to the slow decay of the tail of the distribution function. The analytical prediction (which was not derived in Sec. 3) was virtually indistinguishable on the scale of the graph, which is to be expected because

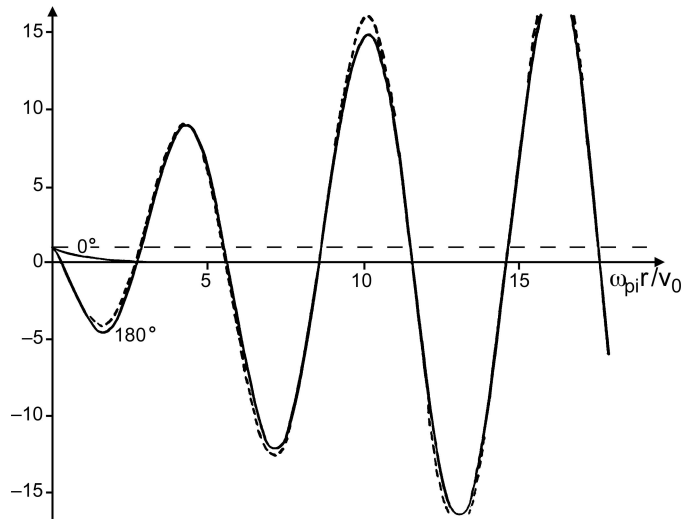


Fig. 11. Plots of  $\varphi(r, \psi)/\varphi_0(r)$  as a function of distance  $r$  (in units of  $v_0/\omega_{pi}$ ) calculated for a test particle moving at  $v_0 = 8\omega_{pi}/k_{Di}$  in a plasma with Maxwellian ions and  $k_{De} = 0$ . The forward field is labelled  $0^\circ$  and the wake field is labelled  $180^\circ$ . The short-dashed curve is the approximation Eq. (3.28).

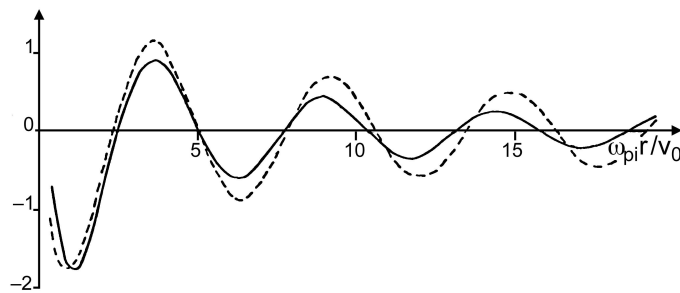


Fig. 12. Same case as in Fig. 11 except that the test particle speed is halved,  $v_0 = 4\omega_{pi}/k_{Di}$ . Plotted is  $[\varphi(r, \psi)/\varphi_0(r)](\omega_{pi}r/v_0)^{-1}$  in the wake,  $\psi = \pi$ .

the dispersion relation is exact.

*Wake field, Maxwellian case:* For a Maxwellian distribution function the agreement with Eq. (3.28) was quite good in the  $v_0 = 8$  case, Fig. 11, but not so good in the  $v_0 = 4$  case, Fig. 12. This may be explained by the inadequacy of the asymptotic expansion Eq. (3.11) when  $|\omega/k| < 4$ . Landau damping may also have some effect.

Owing to computing time limitations the complete wake structure was mapped only in the  $v_0 = 4$  Maxwellian case. A contour plot is given in

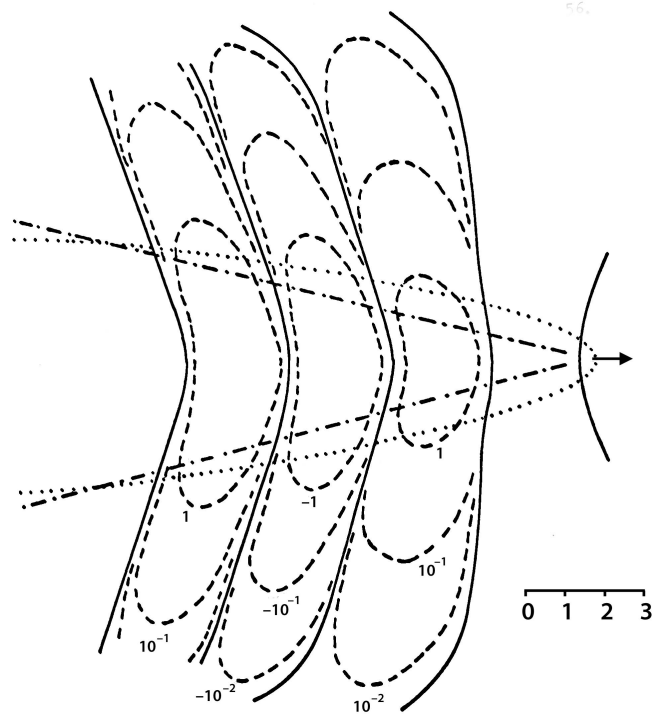


Fig. 13. Contours of  $\varphi(\mathbf{x})/\varphi_0(r)$  for a test particle moving with  $v_0 = 4\omega_{pi}/k_{Di}$  (the direction of  $\mathbf{v}_0$  is indicated by an arrow) in a plasma with Maxwellian ions and  $k_{De} = 0$ . The scale in units of  $v_0/\omega_{pi}$  is indicated lower right, the “thermal Mach cone”  $x_{\perp} = |x_{\perp}|\omega_{pi}/k_{Di}v_0$  is indicated by dash-dotted lines, and the boundary of the region of validity of Eq. (3.35) is indicated by the dotted curve (cf. Fig. 6).

Fig. 13, which represented almost two hours of computing time on the IBM 7044 and is still not very accurate.

#### 4.4. *Supersonic case*

The supersonic case,  $v_0 > C_s$ , considered in Sec. 3.5 was only briefly studied numerically. Figure 14 shows a fairly sharp cutoff near the Mach cone but no shock front. Indeed the function decays monotonically off the axis in complete contrast with the Kraus–Watson<sup>22</sup> result, which predicts an initial increase.



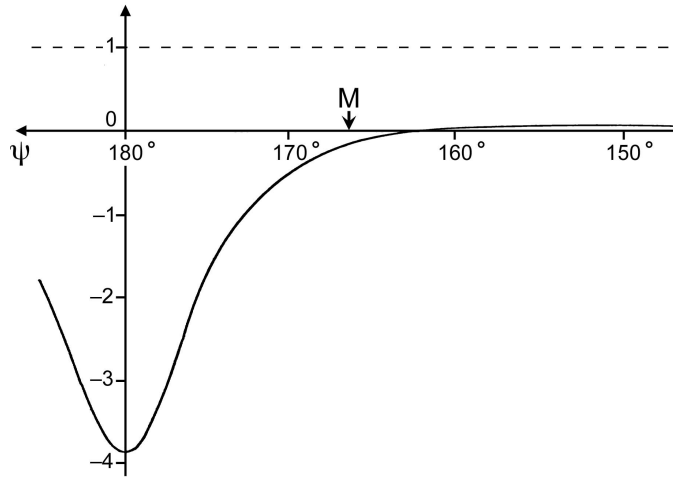


Fig. 14. Plot of  $\varphi(r, \psi)/\varphi_0(r)$  vs.  $\psi$  (with  $r = 48/k_{Di}$ ) in the wake of a supersonic test particle moving at  $v_0 = 32\omega_{pi}/k_{Di} = 4C_s$  in a plasma with  $k_{De} = k_{Di}/8$ . Surprisingly, no shock wave is seen at the expected position of the Mach cone, which is calculated from  $x_{\perp}/|x_1| = \omega_{pi}/v_0 k_{De}$  and indicated by the arrow marked M at  $\psi = 166^\circ$ .

#### 4.5. Conclusion

In the intervening years since my MSc work other authors have made similar calculations. I have not attempted a complete literature search, but note that the research project must have been topical at the time as the inverse third power asymptotic behaviour in Eq. (3.8) was announced a year later by Montgomery, Joyce and Sugihara,<sup>32</sup> in a paper that has been cited 58 times. In fact the problem is even more topical today with the rise of interest in dusty plasmas—for instance the paper by Ishihara and Vladimirov<sup>33</sup> on the wake potential of a dust grain in a plasma with ion flow has been cited more than 80 times.

#### Acknowledgments

I am grateful to Ken Hines for providing an ambiance in which we research students were able to develop intellectually both through his gentle guidance and through mutual interactions. I am indebted particularly to Norm Frankel for indoctrinating me in statistical physics and kinetic theory and sharing his thoughts on many topics, and to Andrew Prentice for many stimulating conversations and for providing the subroutine I adapted for calculating the response function  $\Phi$ .

## References

1. K. C. Hines, Energy distribution of protons due to collision energy loss, *Phys. Rev.* **97**, 1725, (1955). doi: 10.1103/PhysRev.97.1725.
2. L. D. Landau, *J. Phys. (U.S.S.R.)*, **8**, 201, (1944).
3. U. Fano, *Phys. Rev.* **92**, 328, (1953).
4. S. Chandrasekhar, Stochastic problems in physics and astronomy, *Rev. Mod. Phys.* **15**, 1, (1943). Reprinted in "Selected papers in noise and stochastic processes" by N. Wax, Dover, New York, 1954.
5. R. Balescu, *Statistical Mechanics of Charged Particles*. Number 4 in Monographs in Statistical Physics, (Wiley Interscience, London, 1963).
6. D. C. Montgomery and D. A. Tidman, *Plasma Kinetic Theory*. Advanced Physics Monograph Series, (McGraw-Hill, New York, 1964).
7. N. E. Frankel, K. C. Hines, and R. L. Dewar, Energy loss due to binary collisions in a relativistic plasma, *Phys. Rev. A*, **20**, 2120, (1979). doi: 10.1103/PhysRevA.20.2120.
8. R. Balescu, Irreversible processes in ionized gases, *Physics of Fluids*, **3**, 52, (1960). doi: 10.1063/1.1706002.
9. A. Lenard, On Bogoliubov's kinetic equation for a spatially homogeneous plasma, *Annals of Physics*. p. 390, (1960). doi: 10.1016/0003-4916(60)90003-8.
10. W. B. Thompson and J. Hubbard, Long-range forces and the diffusion coefficients of a plasma, *Rev. Mod. Phys.* **32**, 714, (1960). doi: 10.1103/RevModPhys.32.714.
11. J. Hubbard, The friction and diffusion coefficients of the Fokker-Planck equation in a plasma, *Proc. Roy. Soc. (London)*. **A260**, 114, (1961). URL <http://www.jstor.org/stable/2413844>.
12. J. Hubbard, The friction and diffusion coefficients of the Fokker-Planck equation in a plasma. II, *Proc. Roy. Soc. (Lond.)*. **A261**, 371, (1961). URL <http://www.jstor.org/stable/2414287>.
13. N. Rostoker, Superposition of dressed test particles, *Phys. Fluids*, **7**, 479, (1964). doi: 10.1063/1.1711227.
14. R. L. Dewar. Particle-field interactions in a plasma. Master's thesis, University of Melbourne, (1967).
15. R. L. Dewar, Energy-momentum tensors for dispersive electromagnetic waves, *Aust. J. Phys.* **30**, 533, (1977).
16. D. Pines and D. Bohm, *Phys. Rev.* **13**, 338, (1952).
17. S. Rand, *Phys. Fluids*, **2**, 649, (1959).
18. S. Rand, *Phys. Fluids*, **3**, 265, (1960).
19. S. K. Majumdar, *Proc. Phys. Soc.* **76**, 657, (1960).
20. S. K. Majumdar, *Proc. Phys. Soc.* **82**, 669, (1963).
21. M. H. Cohen, *Phys. Rev.* **123**, 711, (1961).
22. L. Kraus and K. M. Watson, *Phys. Fluids*, **1**, 480, (1958).
23. H. A. Pappert, *Phys. Fluids*, **3**, 966, (1960).
24. A. V. Gurevich, *Geomagn. i Aeronomiya (USSR)*, **4**, 3, (1964). English transl. *Geomagn. and Aeronomy (USA)* **4**, 1 (1964).

25. Y. M. Panchenko and L. P. Pitayevsky, *Geomagn. i Aeronomiya (USSR)*. **4**, 256, (1964). English transl. *Geomagn. and Aeronomy (USA)* **4**, 637 (1964).
26. A. V. Gurevich and L. P. Pitayevsky, *Geomagn. i Aeronomiya (USSR)*. **4**, 817, (1964). English transl. *Geomagn. and Aeronomy (USA)* **4**, 637 (1964).
27. A. V. Gurevich and L. P. Pitayevsky, *Phys. Rev. Letters*. **15**, 346, (1965).
28. J. A. Stratton, *Electromagnetic Theory*. (McGraw-Hill, New York, 1941).
29. G. N. Watson, *A Treatise on the Theory of Bessel Functions*. (Cambridge University Press, Cambridge, U.K., 1944).
30. M. Abramowitz and I. A. Stegun, Eds., *Handbook of Mathematical Functions*. Applied Mathematics Series - 55, (National Bureau of Standards, U.S. Government Printing Office, Washington D.C., 1972), 10th printing edition. URL <http://www.math.sfu.ca/~cbm/aands/>.
31. A. Moffat. Fifty years of computing at The University of Melbourne. Department of Computer Science and Software Engineering Department of Information Systems Web Site, (2006). URL <http://www.cs.mu.oz.au/~alistair/fifty-years/mof06history.pdf>.
32. D. Montgomery, G. Joyce, and R. Sugihara, Inverse third power law for the shielding of test particles, *Plasma Physics*. **10**, 681, (1968). doi: 10.1088/0032-1028/10/7/304.
33. O. Ishihara and S. V. Vladimirov, Wake potential of a dust grain in a plasma with ion flow, *Phys. Plasmas*. **4**, 69, (1997). doi: 10.1063/1.872112.